

Polymer-Leather Composites. III. Morphology and Water Absorptivities of Selected Acrylic Polymer-Leather Composite Materials

EDMUND F. JORDAN, JR., ROBERT J. CARROLL, MARY V. HANNIGAN, BOHDAN ARTYMYSHYN, and STEPHEN H. FEAIRHELLER, *Eastern Regional Research Center, Agricultural Research, Science and Education Administration, U.S. Department of Agriculture, Philadelphia, Pennsylvania 19118*

Synopsis

The morphology of composite materials made by polymerizing methyl methacrylate into chrome-tanned cattlehide was examined by both light and scanning electron microscopy. The composites were selected from a series previously prepared and characterized, and their kinetics were reported. Micrographs of the polymer phase of the composites, prepared by preferential removal of collagenous material with 6*N* hydrochloric acid, yielded negative replicas of the fiber conformations. These provided evidence in support of proposed mechanisms of polymer deposition for two different methods of composite preparation. One method involved emulsion polymerization of monomer into hydrated leather and the other, preferentially filling leather free space. Both light and scanning electron microscopy of all composites and replicas revealed poly(methyl methacrylate) deposited largely in coarse aggregates around individual fibers. In emulsion systems, fiber bundles expanded with continuous deposition. No difference was observed in the morphology of bound and deposited polymers. However, high magnification of bound-polymer replicas exposed polymer surrounding some fibril traces. Deposition of polymer in the fine structure of bulk or solution prepared composites was not found; instead, all free space was occupied. A theory specifying polymer location in previous publications of this series, and extended here to define replica parameters, was abundantly supported by measured physical properties. A dominant grafting mechanism was precluded because the large domains limited points of possible attachment. Water absorptivities of emulsion prepared composites and controls were identical when the data were corrected to neat leather, although the rates were slightly perturbed. In contrast, both rate and equilibrium absorption data of the bulk and solution composites were retarded by polymer presence.

INTRODUCTION

This article presents a study of the morphology of composite materials composed of selected acrylate polymers deposited in chrome-tanned cattlehide by free radical polymerization. The investigation also considered the effect of that morphology on rates and equilibrium water absorptivities. As described in a previous article,¹ one method of preparing the composites involved monomer polymerization into the hydrated state of cattlehide; the other, filling the free space of ambient dry cattlehide without matrix expansion. In the former, an emulsion procedure initiated by a redox potassium persulfate-sodium bisulfite combination was used. In the latter, polymer was introduced by polymerizing bulk or benzene diluted monomer in saturated leather panels in a closed system, initiated by azo-bis-isobutyronitrile. Both methods were intended to yield

composite materials having improved plumpness, hydrophobicity, and mechanical properties.¹ Extensive kinetic studies^{1,2} produced little evidence that the bound (unextractable) polymer (about one-half of that deposited) in emulsion systems was produced by a mechanism favoring predominant grafting. The results suggested that the required primary radical attack to out-of-phase substrate in both aqueous and nonaqueous media may be inherently unfavorable for free radical capture because of competing processes for chemical initiation in leather and in other natural fibers described in the literature.³⁻⁷ Consequently, in view of the ambiguities encountered in identifying grafting with bound polymer when deposited in leather,⁸⁻¹⁷ as well as for guidance in characterizing domain sizes and distribution for correlation with future work on mechanical properties,¹⁸ a study of the morphology of the leather composites seemed to be warranted. Further experimental confirmation of an extensive theoretical interpretation of polymer deposit location, set forth in part I¹ of this series, was also desired. In addition, the reason for preferential restriction of deposited polymer to surface layers in emulsion systems was expected to be determined from the morphology observed. The layers comprised about 25-60% of the total specimen thickness (0.23 cm), leaving a center section almost unfilled.

Extensive use has been made of light,¹⁹⁻²¹ transmission, and scanning electron microscopes²² in elucidating the fine structure of polymer composites containing cotton, rayon, and wool. Polymer was found by transmission electron microscopy (TEM) to be distributed throughout the cross-sectional area of cotton²³ and rayon,²⁴ sometimes uniformly,²³⁻²⁶ sometimes in aggregates,²⁷ and sometimes concentrated in growth layers,^{23,28,29} depending on the reaction conditions. These conditions influenced the diffusion characteristics of the monomers²³ when both mutual or preirradiation techniques were employed for producing grafts. For analogous reasons, chemical initiation, such as by use of ceric ion,²³ yielded similar morphologies. In wool, various polymers,^{5,20,21,30} introduced by a variety of chemical means, were observed by TEM to deposit through all regions of the fiber cross section,^{5,31} residing in some cases even around microfibrils³² to produce domains as small as 20 Å thick.⁵ The ultrafine structure of goat skins,¹² investigated by use of TEM, showed gradual elimination of the cross striations of fibrils (650-2000 Å diam), with increasing amounts of *n*-butyl or methyl methacrylate. This was interpreted to indicate that the deposition of the polymer within the fibrils disrupts crystallites.³³ However, because the poly(methyl methacrylate) (PMMA) embedding medium was left in the specimen and the fibrils retained their original diameters, this interpretation remains somewhat in doubt.

In this work, light or scanning electron micrographs are presented for both composites and negative replicas of the corresponding composite matrices. The latter were made by preferential dilute hydrochloric acid etching of the collagen fibers from the composites, leaving an imprint of the fibrous morphology behind in the polymer. The intact, imprinted, continuous plastic phase is referred to in this article as simply a replica. To avoid relaxation of the replica at the high temperature involved during hydrolysis (85-90°C), only the PMMA replicas were examined microscopically. The same systems discussed in part I¹ were studied here. These included PMMA deposited into the matrix by the emulsion polymerization method, and either air dried or methanol extracted to remove water and monomer. Some samples were further extracted with benzene, after methanol extraction, to remove the homopolymer and leave the bound polymer.

For important contrast, homogeneous, unexpanded composites and their replicas were included. These were prepared by bulk or benzene solution polymerization into ambient dry leather panels. To provide a further test of the density theory of part I in estimating replica properties, as well as to establish some lower limit of composite glass transition in avoiding replica distortion, selected (*n*-butyl acrylate-co-methyl methacrylate)-leather composites (BA + MMA) were included. Finally, the hydrophobic influence of the observed morphologies was monitored by studying absorption rates and equilibration absorptivities when the composites were immersed in liquid water. Ranges of compositions were studied in both replication and water absorption measurements.

EXPERIMENTAL

Polymer-Leather Composites

The methods of preparation of these were described in part I.¹ Some were prepared by the same methods specifically for use in future mechanical property evaluation.¹⁸

Replicas

Panels of polymer-leather composites, having dimensions of $12.5 \times 1 \times (0.23-0.30)$ cm, the latter depending on composite thickness, were cut in half and each section was immersed and digested in 6*N* hydrochloric acid ($60 \text{ cm}^3/\text{g}$) at $85-90^\circ\text{C}$ for 5 hr. The mixture was then stored for 15 hr with cooling at room temperature, and the acid was discarded. The process was repeated at 90°C for 1 hr to insure that no color of Cr (III) was being generated (indicating incomplete hydrolysis). The strips, which retained their leatherlike appearance, were extracted 15 times by 15-min immersions each in distilled water ($60 \text{ cm}^3/\text{g}$) or until free of acid by test, blotted to remove loose water, and air dried to constant weight. Some replicas were isolated in two sections (grain and corium) after the composite center layer, which was essentially free of polymer, was split through¹; the combined data were reported. Replicas of *n*-butyl acrylate-leather composites relaxed to sticky shrunken panels that were used only for molecular weight determination.¹

Chemical Properties of the Replicas

Elemental analyses for nitrogen were obtained commercially (Huffman Laboratories)* on all of the replicas. Values never exceeded 0.5 and were usually less than 0.10; the amount of collageneous material remaining in the replicas reached a maximum of 3% but was usually less than 0.6%. The average value for a selected control on an ash and moisture-free basis was 16.79, which is within an acceptable range.¹ Similarly prepared replicas were often soluble in benzene, but many from bound polymer composites contained 20-50% microgel.¹

* Reference to brand or firm name throughout this article does not constitute endorsement by the U.S. Department of Agriculture over others of a similar nature not mentioned.

Light Microscopy

Frozen sections were microtomed at 50, 60, or 100 μm , stained with 0.5% Oil Red-O in isopropanol for 4–6 hr to insure color penetration through the polymer phase, mounted from distilled water in glycerine jelly, and photomicrographed with a Zeiss photomicroscope at 40 \times , with 3 \times enlargement in printing. The Oil Red-O was specific for the polymer phase.

Scanning Electron Microscopy

Cross sections of the leather and replica samples were cut and mounted on copper stubs with a minimum of silver paint. To minimize charging, the samples were coated with a thin layer of gold (~ 15 nm) with a Denton DSM-5 cold sputter module. The electron micrographs were obtained with a JEOL JSM 50A operating at 15 kV.

Liquid Water Absorption

Analytically weighed samples of composites of 1–3 g were suspended under distilled water for predetermined times of 1 sec to 8 days. Samples were removed, padded dry, analytically weighed, and returned to the water. Except for sample size and geometry, this method is close to a standard procedure for leather³⁴ and resembles a swelling capacity procedure for cotton.³⁵

Surface water absorption was obtained by noting the time of disappearance of one drop of water released from a 2-ml syringe onto the grain surface of composites and their controls. No correction was made for evaporation error, which became important after 10 min.

Definitions and Leather Constants

Terms used in parts I¹ and II² are used here; new terms, specific to this article, are defined in the text. Reference to the composite systems are by monomer used as methyl methacrylate (MMA); *n*-butyl acrylate-co-methyl methacrylate (BA + MMA); and *n*-butyl acrylate (BA). Composite and leather constants were taken from Table III of part I. Attention was given to comparing micrographs of composites and replicas in the various figures at similar locations in the cross section (often designated by the word corresponding). However, pictures of the exact location in both composite and replica were never obtained; even when magnification was increased for the same system, correspondence was not exact, unless so stated in the text. Relative magnification used in this work is defined as low, 40–50 \times (mostly light microscopy); intermediate, 300–1000 \times (SEM); high, 10,000 \times (SEM). An IBM 1150 computer was used for curve fitting.

RESULTS AND DISCUSSION

Replica Density and Volume Distortion

All composites and replica densities, specimen thicknesses, and estimates of the fractional extent of shrinkage of the corresponding replicas collected in this work are listed in Table I. Density of all of the replicas was less than that of the

TABLE I
Composite and Replica Densities, Replica Thickness, and Extent of Shrinkage

Experi- ment No. ^a	Sys- tem ^b	Com- posite ω_2^c	Composite density		Replica density		Replica thickness		Fractional extent of replica shrinkage ^g	
			ρ_a calc., ^d g cm ⁻³	ρ_a found, g cm ⁻³	ρ_d calc., ^e g cm ⁻³	ρ_d found, g cm ⁻³	h_d calc., ^f cm	h_d found, cm	V_r/V_{r0}	v_f/v_{f0}
Poly(methyl Methacrylate)-Leather Composites and Replicas										
1*	A	0.447	0.759	0.769	0.490	0.483	0.198	0.248	0.938	0.826
2		0.335	0.701	0.643	0.363	0.345	0.181	0.225	0.900	0.916
3		0.203	0.642	0.599	0.236	0.326	0.145	0.160	0.783	0.865
4		0.0894	0.598	0.563	0.104	0.280	0.131	0.158	0.458	0.774
5*	B	0.470	0.772	0.775	0.543	0.453	0.207	0.242	0.995	1.02
6		0.347	0.707	0.655	0.402	0.381	0.172	0.171	0.963	1.03
7		0.258	0.711	0.636	0.300	0.308	0.150	0.172	0.942	0.938
8		0.182	0.633	0.633	0.212	0.250	0.133	0.134	0.871	0.949
9*	C	0.423	1.082	1.081	0.535	0.423	0.186	0.237	1.031	0.995
10		0.292	0.934	0.948	0.272	0.288	0.199	0.204	0.989	0.975
11		0.234	0.851	0.874	0.199	0.219	0.208	0.193	1.010	0.995
12*		0.189	0.795	0.793	0.145	0.180	0.195	0.183	0.942	0.977
13		0.155	0.758	0.780	0.118	0.202	0.228	0.155	0.768	1.01
14*	D	0.447	0.747	0.752	0.517	0.433	0.152	0.179	1.014	1.01
15		0.366	0.711	0.695	0.424	0.410	0.160	0.141	1.035	0.955
Poly(<i>n</i> -Butyl Acrylate-co-Methyl Methacrylate)-Leather Composites and Replicas										
16	B	0.588	0.821	0.739	0.620	0.773	0.234	0.174	1.081	1.097
17		0.389	0.724	0.698	0.512	0.489	0.161	0.124	1.303	1.230
18		0.280	0.675	0.643	0.436	0.420	0.106	0.0953	1.074	1.090
19		0.184	0.633	0.632	0.404	0.262	0.0691	0.0565	0.857	0.821
20		0.0875	0.592	0.626	0.405	0.518	0.0319	0.0565	0.511	0.446
21	C	0.467	1.103	0.996	0.552	0.661	0.154	0.142	0.910	0.901

^a Those marked with an asterisk were studied in SEM and light microscopy.

^b Designations are (A) emulsion-prepared composite, methanol and benzene extracted; (B) emulsion-prepared composite, methanol extracted only; (C) solution-polymerized composite; (D) emulsion-prepared composite, then air-dried.

^c Weight fraction of polymer in the composite.

^d Eq. (4).

^e Eq. (8).

^f Eq. (10).

^g V_r = replica, $lwh_{\text{calc.}}$; V_{r0} = composite $lwh_{\text{calc.}}$; v_f/v_{f0} eq. (14).

corresponding composites, as would be expected when collagen is removed in the absence of relaxation. Density for both composites and their replicas decreased with decrease in polymer content. The magnitude of the densities of the replicas for the emulsion systems, where layers were found in the original composite, was greater than bulk or solution prepared replicas of the same composite w_2 , which were homogeneous. This demonstrates that the higher concentration of polymer in the layers more than compensated for the reduced volume of free space available to the unexpanded bulk compositions at similar w_2 .¹ This is also apparent from the greater thickness of the latter replicas. The

replicas of all systems, except MMA, experiments 3 and 4 and BA + MMA of $\omega_2 \leq 0.18$, showed little shrinkage during preparation (last two columns), thus insuring that, in general, the replicas duplicated the morphology of the original composite.

The theoretical relationships between composite and replica parameters, in view of a previous discussion,¹ are relevant to a visual description of replica morphology and extent of distortion. Thus, this analysis should provide a conceptual basis for interpreting the micrographs presented later. These relationships are discussed in the next section.

From the analysis of density presented in part I¹ of this series,^{1,2} the volume of 1 g of composite panel, $(W_1 + W_2)$ prepared by homogeneous polymer deposition from emulsion is given by

$$V_t = V_1 + V_2 + V_a(\rho_{ao}/\rho_i) = W_1/\rho_r + W_2/\rho_p + v_{fo}(W_1/\rho_{ao})(\rho_{ao}/\rho_i) \quad (1)$$

where w_i and ρ_i are weight fraction and density, respectively, and V_a is the total volume of free space present in the leather. In eq. (1), $W_1 = w_1(W_1 + W_2)$ and $W_2 = w_2(W_1 + W_2)$. Weight fraction and volume V_i are designated by numbered subscripts as (1) leather and (2) polymer, respectively. Densities are designated by lettered subscripts as r , real¹; p , synthetic polymer; a , apparent, while v_f and v_{fo} are volume fractions of free space, the latter for the initial untreated leather. The ratio ρ_{ao}/ρ_i is a small correction factor¹ for the assumed initial filling of small pores. Assuming no relaxation of the polymer phase on removal of collagen by hydrochloric acid, so that the polymer would truly reflect details of the fibrous structure originally present, the total volume of the replica can also be equated to V_t . However, since V_1 was removed, total replica free space, V_F , becomes

$$V_F = V_1 + v_{fo} V_a(\rho_{ao}/\rho_i) = W_1/\rho_r + v_{fo}(W_1/\rho_{ao})(\rho_{ao}/\rho_i) \quad (2)$$

Thus, density of the replica, ρ_d , is

$$\rho_d = W_2/(V_F + V_2) = W_2/(V_F + W_2/\rho_p) \quad (3)$$

To account for the preferential deposition of polymer in the outer regions of the leather panel (the layer effect) the layer density, ρ_1 , can be computed¹ by

$$\rho_1 = 1/[W_1'/\rho_r + W_2'/\rho_p + (v_{fo}W_1'/\rho_{ao})(\rho_{ao}/\rho_i)] \quad (4)$$

where

$$w_2' = (1/W_1 - 1)/[v_2^* + (1/W_1) - 1] \quad (5)$$

and

$$w_1' = 1 w_2' \quad (6)$$

and where v_2^* is the layer fraction. In eq. (4), $W_2' = (W_1 + W_2)w_2'$ and $W_1' = (W_1 + W_2)w_1'$. The layer fraction, v_2^* , usually varies from 0.25 to 0.60, depending on reaction time and the monomer used,¹ although for MMA deposition the value was 0.5. After destruction of the collagen in layered composites, the volume of free space accruing to the replica, V_F' , is now

$$V_F' = W_1'/\rho_r + v_{fo}(W_1'/\rho_{ao})(\rho_{ao}/\rho_i) \quad (7)$$

so that density of the resulting replica becomes

$$\rho_d' = W_2'/(V_F' + W_2'/\rho_p) \quad (8)$$

It follows that the volume, V_d , of 1g of the replica is

$$V_d = 1/\rho_d' \quad (9)$$

having a thickness, h_d , of

$$h_d = V_d/lw = V_d/A \quad (10)$$

where A is the original experimental composite area, corrected to 1 g, by use of $(lw)_0/W_2$, with $W_2 = w_2(W_1 + W_2)$, and $W_1 + W_2$ the composite weight.

By similar reasoning, the total free space, V_F , of the replicas made from bulk or solution polymerization can be estimated. In these systems, the polymer was shown¹ to fill only the leather open space, so that V_F follows

$$V_F = W_1/\rho_r + [v_{fo}(W_1/\rho_{ao}) - (W_2/\rho_p)(\rho_r/\rho_p)] \quad (11)$$

and thus the available space is depleted rapidly compared to that of the emulsion system, eq. (7). This follows from the form of their densities¹

$$\rho_a = 1/(W_1/\rho_r) + (W_2/\rho_p) + v_{fo}(W_1/\rho_{ao}) - (W_2/\rho_p)(\rho_r/\rho_p) \quad (12)$$

The other quantities, V_d , h_d , V_r/V_{ro} , and v_f/v_{fo} , remain the same as for the emulsion systems. The extent of actual relaxation of the continuous polymer matrix in all replicas, compared to that in the original composite, was estimated by

$$V_r/V_{ro} = lwh_d/(lw)_0h_d = A/A_o \quad (13)$$

where h_d is from eq. (10). The areas A and A_o are those found for the replicas and their composites, respectively. Calculated values of h_d were preferred for accuracy because the extreme fragility of the replicas made accurate thickness measurements difficult. An alternate criterion for measuring replica distortion comes from ratios of the volume fraction of free space, given by

$$v_f/v_{fo} = (V_a/V_t)_{\text{experimental}}/[V_F'/(V_F' + W_2'/\rho_p)] \quad (14)$$

The close agreement found in Table I for both calculated and observed composite and replica densities and derived quantities for such a large number of samples provides confidence that the original analysis and its present modification are essentially correct. It was postulated initially,¹ in analogy with experience from cotton and wool,^{5,20-31} that polymer is deposited from emulsion near fibrils in the ultrafine structure of fibers, thus expanding fibers and their fiber bundles to produce the increased composite volumes compared to their controls. This was amended² to include the equivalent concept that polymer concentrates in much larger domains around fibers²² to merely expand fiber bundles. From the micrographs presented in the following material, a choice between these extreme positions should be ascertainable for the emulsion method of composite preparation. The crude space-filling postulate predicted for bulk or solution deposition should also be verifiable. For convenience in comparing the deposition intimacy for polymer-treated natural fibers present in the literature,^{5,22-29} approximate values for arbitrary aggregation levels are offered in Table II.

TABLE II
Relative-Size Aggregation for Natural Fibers

Aggregation level ^a	Cotton ^b	Wool ^c	Leather ^d
1	10 μm diam; cellular	14 μm diam; multicell	fiber bundles, 15–200 μm
2	macrofibril, 0.4 μm diam	cortical cell, 3–6 μm diam	fibers, 1.5–5 μm diam
3	microfibrils, 250 \AA diam	macrofibrils, 650–2000 \AA	fibrils, 650–2000 \AA
4	elementary fibrils, 35 \AA	microfibrils, 70 \AA diam	protofibrils, 35 \AA
5	cellulose, 4 \times 8 \AA	protofibrils, 30 \AA diam	tropocollagen, 15 \AA
6		triple helix, 15 \AA diam	

^a These levels are purely arbitrary and are given for convenience only. The existence of many of the smallest aggregates is controversial and the size ranges for all vary more than indicated. However, the basic natural building units for cotton, wool, and leather are at level 3.

^b Ref. 36.

^c Ref. 32.

^d Refs. 33 and 37.

Light Microscopy

Light microscope (LM) micrographs in Figure 1 show the untreated 5-oz chrome-tanned crust cattlehide used as the substrate for polymer modification and for controls. Figure 1(a) depicts the grain area (top), close to the epidermis, and the transition region (below) between the grain and corium region. Also shown are characteristic histological features, such as a portion of a hair follicle (lower center), fatty deposits, and fragments of capillaries, nerves, and muscles (dark irregular shades). Densely packed fiber bundles of the smallest sizes found in leather (Table II), oriented generally parallel to the surface are typical of the grain region. Figure 1(b) shows the much thicker, interweaving fiber bundles (Table II) that characterize the corium region. The generally planar bundles

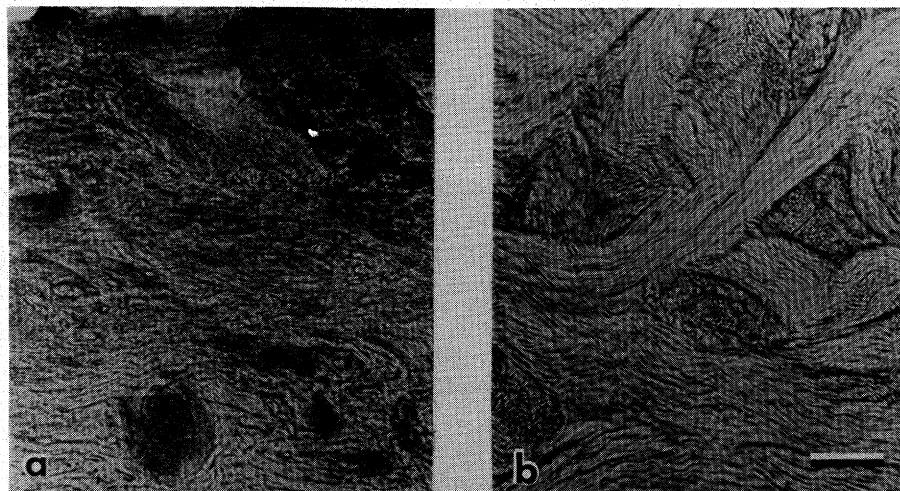


Fig. 1. Light microscope (LM) micrographs of untreated 5-oz chrome-tanned cattlehide (control) showing cross sections of portions of the grain layer (a) and the corium layer (b). The lower half of (a) is the grain–corium interface region. The dark circular area is the root of a hair follicle; the other irregular dark areas are fragments of capillaries or fatty deposits. Scale 100 μm .

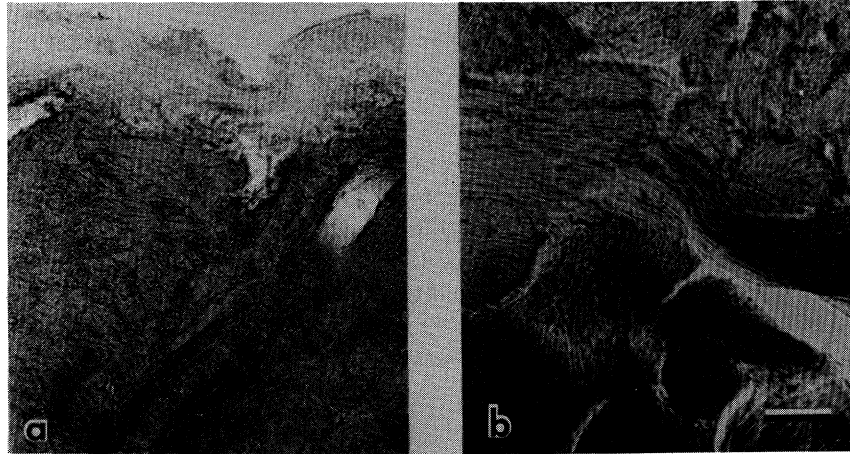


Fig. 2. LM micrographs of a cross section of bound polymer-leather composites prepared in emulsion (Table I, experiment 1) showing cross sections of the grain layer (a) and the corium layer (b). The light region at the top of (a) is the clear zone discussed in the text. Scale 100 μm .

are interspersed with bundles oriented normal to the picture plane. The weaving striations, running parallel but often tilted with respect to the picture plane, and small protrusions, normal to the plane, are individual fibers. Figure 2(a) presents micrographs of cross sections of the grain region and Figure 2(b) shows the corium region for an emulsion prepared, bound polymer composite, experiment 1, Table I. The dark area in Figure 2(a) is stained polymer; the clear area at the top, near the grain surface, is free of polymer. As has been pointed out,¹ it is not known at present why this region, which is most exposed to invading polymer particles and polymerizing monomer,² remains seemingly polymer-free. The plasticlike character of the coated fibers in Figure 2(b) contrasts with the appearance of the untreated corium section in Figure 1(b). Figure 3 presents micrographs of

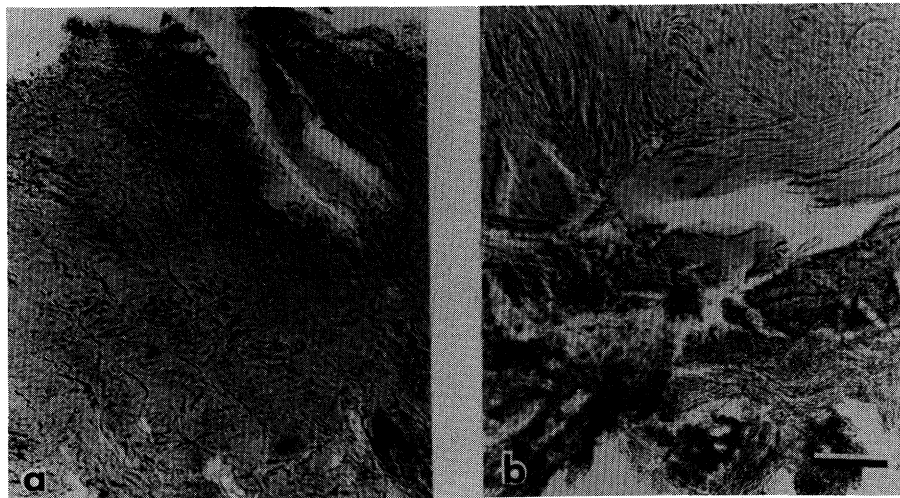


Fig. 3. LM micrographs of the cross sections of the replicas prepared by hydrochloric acid etching of the composites of Fig. 2: (a) the grain layer; (b) the corium layer. Scale 100 μm .

replicas corresponding to the composites of Figure 2. Both were taken close to their respective surfaces. In both regions [Fig 3(a) and 3(b)] the polymer phase is continuous at macrodimensional levels, and the histological characteristics of Figure 1 are essentially preserved. When less bound polymer was present (Fig. 4), the corium fibers of the composite [Fig. 4(a)] show a more leatherlike appearance. A transition between the composite lower region of the micrograph and the untreated region (top) can be noted. This illustrates a typical boundary between layers. The replica [Fig. 4(b)] is somewhat more transparent than in Figure 3(b), in line with its lower density (Table I). Bulk polymerized composites [Fig. 5(a)] appear more densely packed than those prepared in emulsion [Fig. 2(b)] reflecting polymer presence in the gross free space,¹ while their replicas [Fig. 5(b)] show large cavities and a coarser texture induced when collagen was

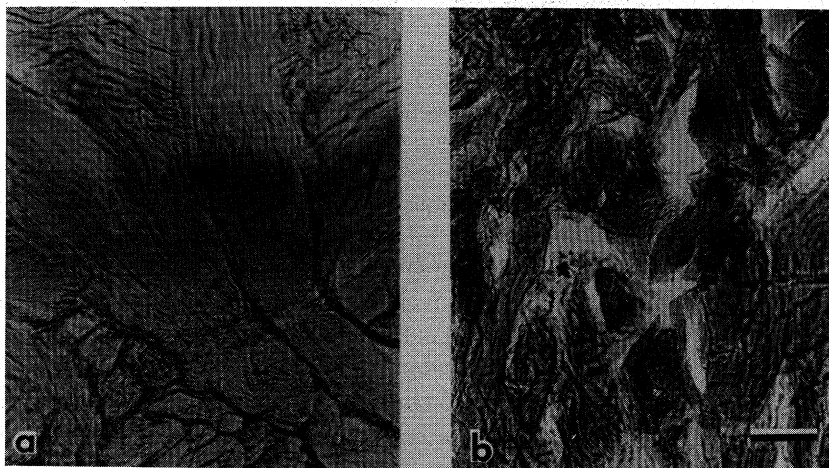


Fig. 4. LM micrograph of (a) the cross section of a bound polymer-leather composite prepared in emulsion (Table I, experiment 3). The light area at the top of the figure is an untreated layer of corium; the bottom section is the composite. (b) a corresponding corium replica cross section. Scale 100 μm .

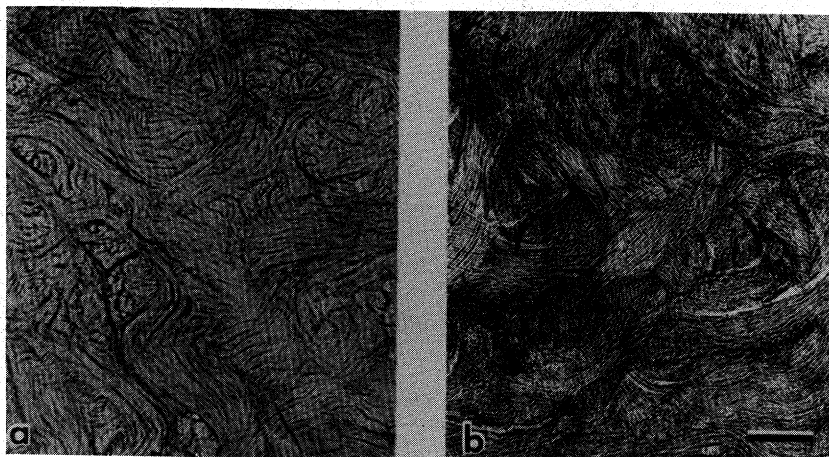


Fig. 5. LM micrographs of (a) the cross sections of a bulk prepared polymer leather composite from the corium region (Table I, experiment 9) and (b) corresponding replica cross section. Scale 100 μm .

removed. A less dense appearance for a solution-prepared composite containing less polymer [Fig. 6(a)] and a finer grained texture for its replica [Fig. 6(b)] are seen, compared to those pictured in Figure 5.

Thus, low magnification ($\sim 40\times$) light microscope micrographs for composites made by both types of preparation method reproduce in the polymer phase histologic features of the original leather-fibrous matrix. This requires that much of the polymer be coarsely deposited in fused aggregates to create a continuous phase that essentially surrounds the fibers. This broad generalization is confirmed and a more detailed description is furnished for these composites and replicas by the greater resolving power of scanning electron microscopy in the following sections.

Scanning Electron Microscopy

A scanning electron micrograph (SEM) at low magnification [Fig. 7(a)] shows about 70% of the cross section (~ 0.24 cm) of an untreated control sample. This

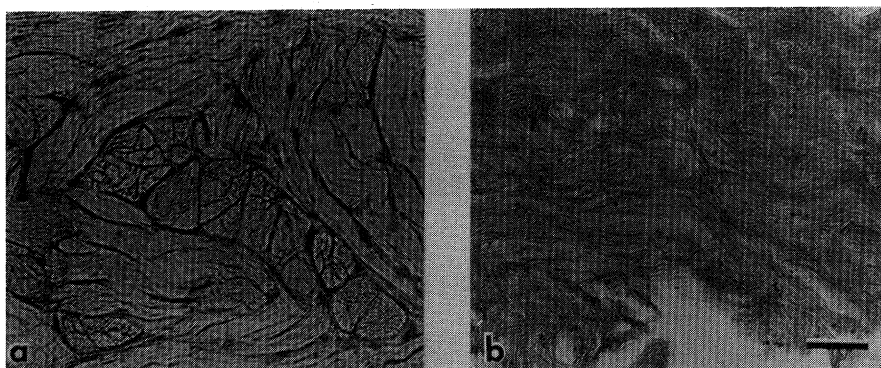


Fig. 6. LM micrographs of (a) the cross section of a solution prepared polymer-leather composite containing a smaller polymer weight fraction than that of Fig. 5 (Table I, experiment 12) and (b) a corresponding replica. Scale $100\ \mu\text{m}$.

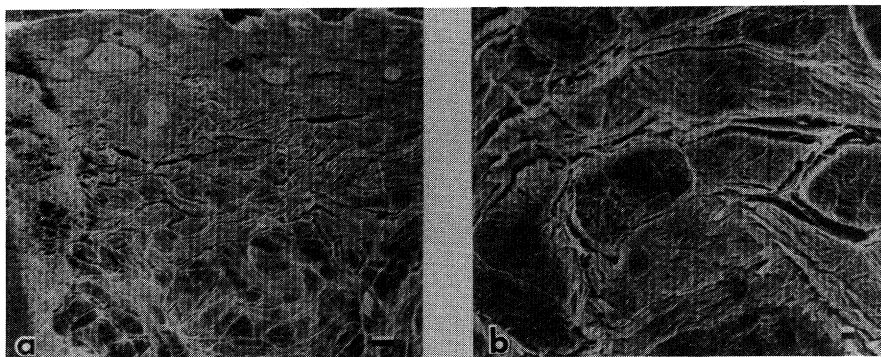


Fig. 7. Scanning electron micrographs (SEM) of the cross sections of untreated 5-oz chrome-tanned cattlehide (control). (a) Low magnification cross section (scale $100\ \mu\text{m}$) showing the fine, tightly packed grain layer in the upper one-third of the photograph and the larger, well-defined fiber bundles, characterizing the corium layer below. (b) Higher magnification (scale $10\ \mu\text{m}$) cross section of the corium fiber bundles showing individual fibers of $1.5\text{--}4\ \mu\text{m}$ diam.

image reveals the finely textured, closely packed grain layer (top) and the coarser cross section of normal, elongated, and tilted fibers that aggregate in bundles and constitute the fibrous matrix. Individual fibers of the corium ($1.5\text{--}4\ \mu\text{m}$) (Table II) can be seen at intermediate magnification ($300\times$) in Figure 7(b). The irregularity in size and shape of the fiber bundles is apparent. A SEM [Fig. 8(a)] of the corium region of bound polymer composites for the same system already seen by light microscopy [Fig. 2(b)] shows the packed, compressed features and expanded fiber bundles produced by PMMA surrounding individual fibers in each of the fiber bundles. When collagen was removed [Fig. 8(b)], holes and tubular apertures of sizes ($1.5\text{--}4\ \mu\text{m}$, Table II) corresponding to the initial fiber dimensions were retained, encased in polymer. This is better seen in Figure 9 at a slightly higher magnification ($1000\times$) where untreated fibers [Fig. 9(a)] have dimensions close to the apertures in the replica [Fig. 9(b)]. This suggests that little polymer penetrated to the aggregation level of fibrils here (Table II); if it had, the holes might be expected to be larger. However, all of the replicas that duplicated the emulsion polymer morphology in this work were not tubelike porous structures, as in Figures 8 and 9. Figure 10 shows more typical mor-

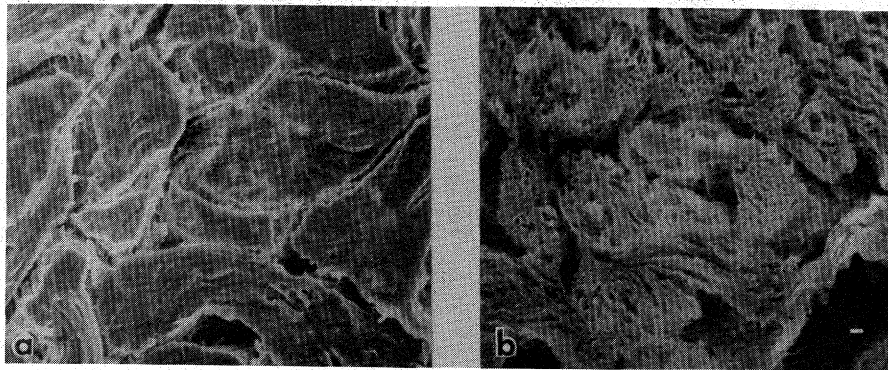


Fig. 8. SEM of (a) cross section of bound polymer-leather composites, prepared in emulsion (Table I, experiment 1) and (b) the corresponding replica prepared by hydrochloric acid etching, showing the effect of removing the collagenous material selected from similar regions of the corium. Scale $10\ \mu\text{m}$.

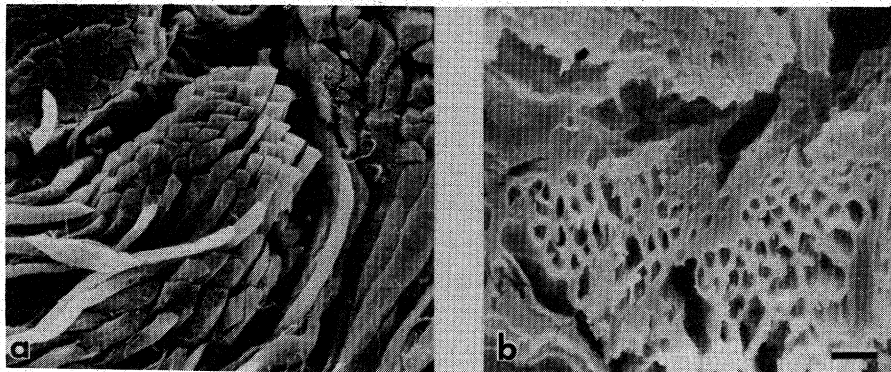


Fig. 9. SEM of (a) a cross section of untreated leather at higher magnification ($1000\times$) than that of Fig. 7, and (b) $300\times$ compared with a typical section of the bound polymer replica of Fig. 8(b). Fiber diameters correspond approximately to replica openings; the polymer is largely confined to the fiber bundle. Scale $10\ \mu\text{m}$.

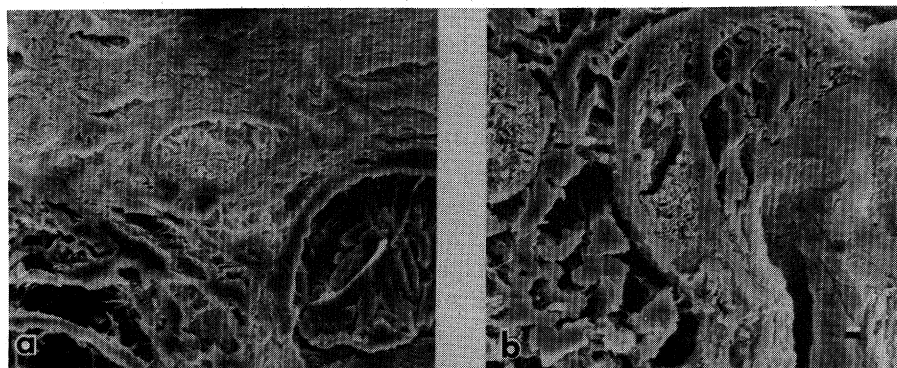


Fig. 10. SEM (Table I, experiment 3) of the cross section of (a) a bound polymer-leather composite showing the grain (top), corium (bottom) interface, and (b) a section of the replica corresponding to a similar interfacial location. Scale $10\ \mu\text{m}$.

phology; these are micrographs of the bound polymer of lower polymer content (Table I, experiment 3). The grain-corium interface of the composite [Fig. 10(a)] shows the packed fibers encrusted with polymer. A replica of the same region [Fig. 10(b)] shows solid appearing masses of $10\text{--}50\ \mu\text{m}$ surrounding porous features that at times are less than the usual fiber dimensions. In fact, the micrographs obtained for the replicas in this work constitute such a bewildering variety of different fiberlike and randomly convoluted conformations that examples of all types cannot be presented. For example, Figures 11(a) and 11(b) are micrographs of the cross section of a replica of the corium region of deposited polymer that had been isolated by treatment with methanol at ambient temperature only.¹ Clusters of partially coalesced individual polymer-emulsion particles appear to be hanging on fused polymer masses of much larger dimen-

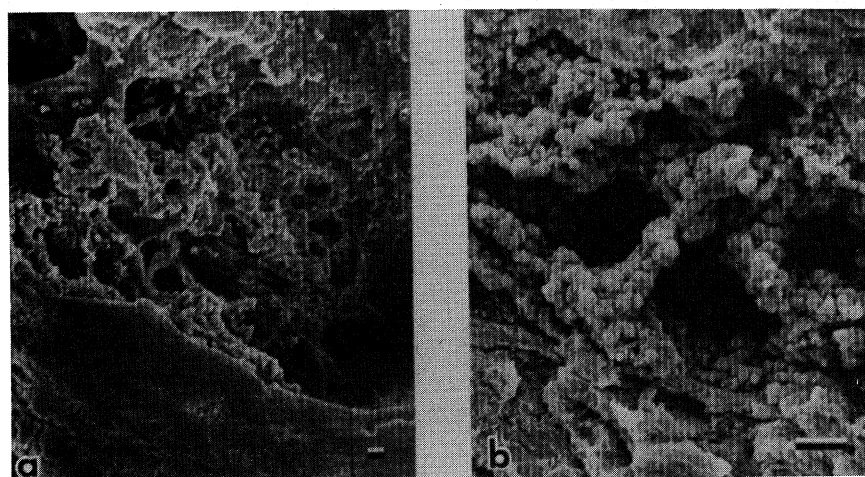


Fig. 11. SEM of the cross section of a replica composed of deposited polymer, extracted with methanol only (Table I, experiment 5). (a) A section of the corium showing clusters of partially coagulated polymer particles adhering to fused polymer aggregates. (b) Another location of the replica at higher magnification ($1,000\times$). Scale $10\ \mu\text{m}$; polymer particles measure $2,000\text{--}10,000\ \text{\AA}$ diam.

sions. These are, in turn, perforated by holes remaining after fiber digestion. The particles can be seen better at higher magnification (1,000 \times) but in a different location in Figure 11(b) than in Figure 11(a). Extraction with a nonsolvent at room temperature appeared to have preserved some of the particles. In contrast, benzene extraction (Figs. 8–10), which swelled the composite considerably, probably obliterated all traces. When the original composites were merely air dried after preparation particles of the same size (2,000–10,000 Å diam) were seen on porous replicas (Fig. 12). These large particle sizes³⁸ are in harmony with the rather unstable emulsion recipe² adopted for this process of leather modification.^{13–16} Aggregation of monomer swollen polymer particles has been postulated from kinetic results² to be an important, but not exclusive, method of polymer deposition in these emulsion systems. Transport of the monomer by diffusion through the continuous polymer phase to occluded radicals constituted another important means. The morphology shown in these micrographs is not at variance with this mechanism.

Most of the polymer introduced in leather by the emulsion process¹ was deposited in large aggregated masses at least 4–20 μm thick and sometimes greater (Fig. 10). Much of this was clustered around fibers to expand fiber bundles. This, in turn, expanded the matrix to increase the composite volume with increase in polymer content, as was postulated theoretically in part I.¹ The space between fiber bundles appeared to be preserved; this is in harmony with the rate of change of the free space in the composites [eq. (1)] and replicas [eqs. (2) and (7)] with increase in polymer composition of the composites. No difference could be detected from the micrographs between polymer bound and that merely deposited. This similarity, together with the large number of polymer coils that must exist between attachable sites, as is apparent from the micrographs, lends little support to a dominant grafting mechanism. The morphology of bulk and solution prepared composites and replicas, where grafting is unlikely,^{1,39,40} adds support to these conclusions.

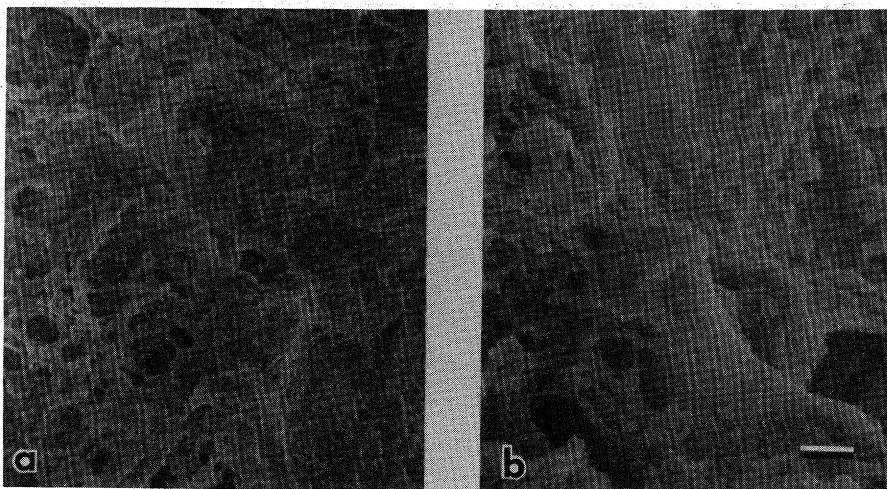


Fig. 12. SEM of the cross section of the replica of a deposited polymer-leather composite that was not extracted but only air dried (Table I, experiment 14) taken from the bottom of the corium region. Micrographs (a) and (b) represent different magnifications of the same region. (b) Depicts the upper-left-center peak in (a). Clustered spheres are polymer particles 2,000–10,000 Å diam.

Figures 13–15 show micrographs of composites (a) and their replicas (b) for selections (Table I) made by bulk and solution polymerization. In the corium region, at high polymer concentrations [Fig. 13(a)] the tightly packed polymer (Table I, experiment 9) obscures fibers even in cross sections; at lower concentrations [Figs. 14(a) and 15(a)] the deposition is less dense and resembles more closely the bound polymer emulsion system in Figure 8(a). The corresponding replicas also illustrate the effect of polymer concentration. At high polymer concentration [Fig. 13(b)] fiber-sized openings are embedded in poly(methyl methacrylate) that even fills the space around fiber bundles. This behavior was anticipated by eqs. (11) and (12) in part I.¹ At lower MMA concentrations [Figs. 14(b) and 15(b)], a much more porous morphology is apparent in both grain and corium replicas in further agreement with eq. (11) (Table I).

The foregoing micrographs from both light and scanning microscopy permitted examination of MMA composites and replicas at relatively low magnification (to 1000 \times); the ultrafine structure remains to be investigated to determine if polymer had penetrated into interfibrillar space and beyond (Table II). Figures 16 and 17 present high-magnification micrographs (10 000 \times) of random selec-

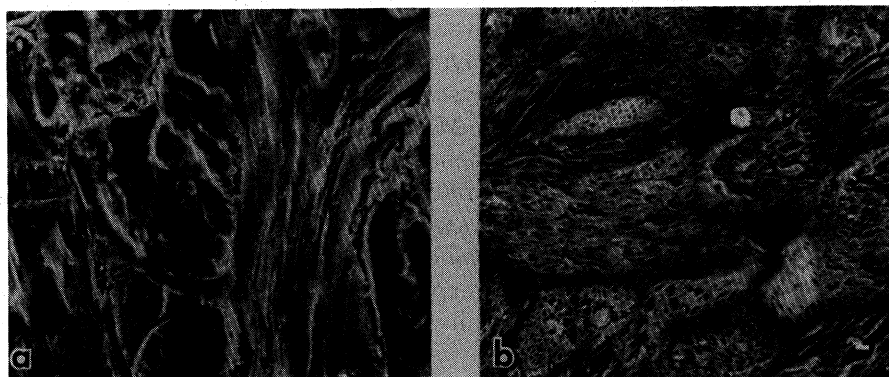


Fig. 13. SEM of (a) the cross section of the corium region of a bulk polymerized polymer-leather composite (Table I, experiment 9) and (b) a replica of an adjacent location of the same material. Holes visible in (b) correspond to fiber diameters 1.5–5 μm . Scale 10 μm .

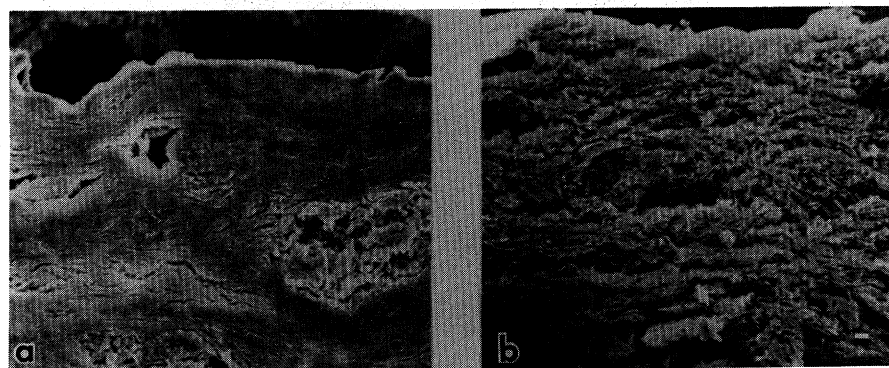


Fig. 14. SEM of (a) the cross section of the grain layer of a polymer-leather composite containing less polymer than in Fig. 13 (Table I, experiment 12) and (b) a replica of a similar location of the grain layer. Scale 10 μm .

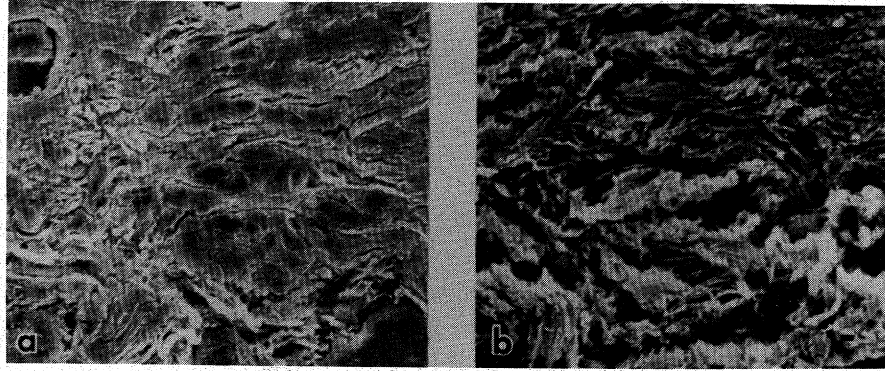


Fig. 15. SEM of (a) the cross section of the corium layer of a bulk polymer-leather composite containing a small amount of polymer (Table I, experiment 12) and (b) a replica of a similar location of the corium layer. Scale is $10\ \mu\text{m}$.

tions from a corium replica of an emulsion-prepared bound polymer composite, experiment 1, Table I. Figures 16(a) and 16(b) clearly show tunnels corresponding to fibril diameters ($500\text{--}2000\ \text{\AA}$, Table II) defined by a very thin, $300\text{--}800\ \text{\AA}$, coating of polymer. However, other sections of the replica (Fig. 17), while monitoring finely structured polymer [Fig. 17(a)], also contain openings [Fig. 17(b)] of fiber dimensions, circumscribed by tubular striations of fibrillar dimensions. This suggests that some MMA penetrated ununiformly into the ultrafine regions during the emulsion deposition process. However, most of the polymer was coarsely packed in interfiber space because (from the preceding micrographs) the amount of polymer seen in replicas relative to that in composites qualitatively matches the initial composite composition (Table I). In addition, Figure 8 revealed little fiber expansion. Hydration of the leather appeared to be required to assist the small extent of interfibrillar deposition that

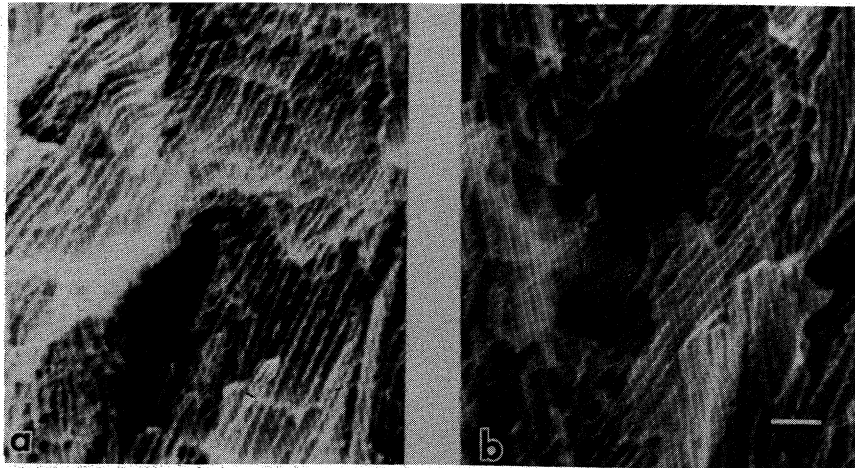


Fig. 16. High magnification ($10,000\times$) SEM of the cross section of the corium region of a replica of a composite (Table I, experiment 1). Micrographs (a) and (b) were taken from different positions in the replica. The linear hollow tubes are $\sim 500\text{--}2000\ \text{\AA}$ diam and correspond to the dimensions of fibrils. Scale $1\ \mu\text{m}$.

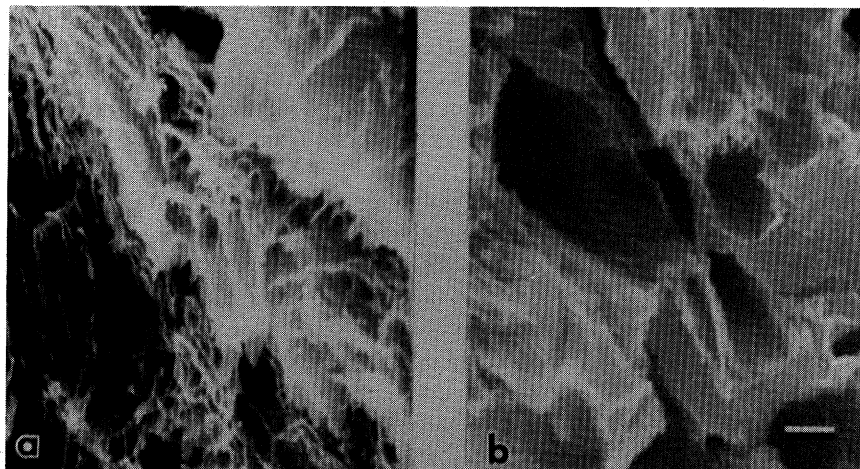


Fig. 17. The same as Fig. 16 but from different locations of the replicated corium.

was actually observed. Cross sections of replicas made from bulk composites [Figs. 18(a) and 18(b)] show no interfibrillar deposition, except for that appearing as striations at fiber boundaries.

These micrographs appear to substantiate the mechanism presented in parts I and II for the nucleation and growth of the polymer phase as deposited from both emulsion and solution into the leather matrix. For the emulsion systems, polymer particles were believed to enter from the float (aqueous phase) in the early stages of polymerization, become unstable, and coagulate to form nuclei of polymer aggregates restricted to the outer regions of the leather panel. These then mixed with unstable growing oligomer particles precipitating from the inner aqueous phase, according to the concepts of Fitch and Tsai⁴¹ and others.⁴² Monomer diffused from the monomer droplets³⁸ at a fixed rate, largely through

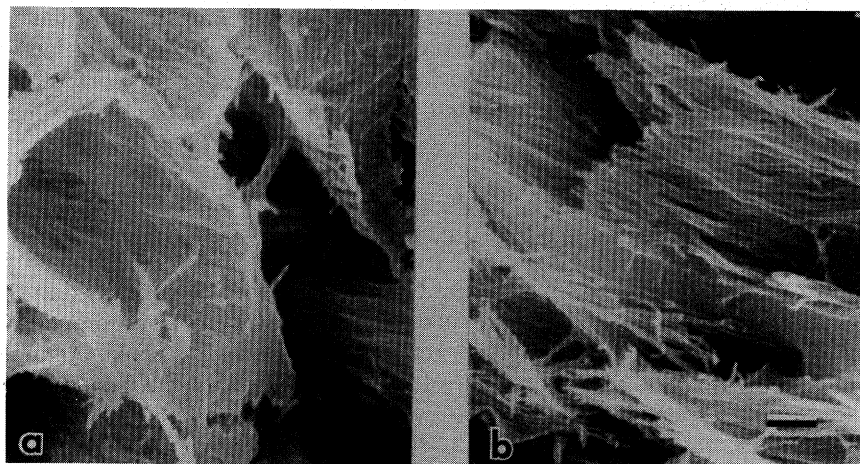


Fig. 18. High magnification SEM of the cross section of a replica of a bulk polymerization composite (Table I, experiment 9). Micrographs (a) and (b) were taken from different locations of the corium region and are typical of the whole. Surface irregularities around fiber tubes are of fibrillar dimensions 500–2000 Å. Scale 1 μm .

this polymer phase,² to nascent and occluded radicals present in and on polymer surfaces. Deposition continued there to produce polymers of molecular weight greater than that produced in the float. An extension of this process probably allowed some polymer to penetrate even to the fibril region because the hydrated matrix was expanded. Polymer could also deposit from the aqueous phase into microfibrillar regions.

The relatively coarse deposition of polymer into leather by emulsion and solution method contrasts with the intimate morphology of polymer-treated cotton²³ and wool.⁵ Polymer often deposited around the microfibrils (Table II) of cotton fibers in aggregates around 200–500 Å thick^{23–26} for composites prepared by mutual or preirradiation techniques. However, some polymers were limited to growth layers,^{23,28,29} forming aggregates 1000–5000 Å in cross section and, with MMA, was limited to dense layers,²³ but these could support considerable graft density. Acrylonitrile polymerized around the macrofibrils of wool fibers in Fe²⁺/H₂O₂ initiated systems³¹; but, in a special case exhibiting assured grafting,⁵ penetration of PMMA to the microfibrillar level (Table II) appeared to have taken place. For polymer-treated cotton fabric, SEM revealed the appearance of some surface polymer.²² However, TEM presented a morphology fine enough within the fiber to support considerable grafting.

The influence of the morphology of MMA polymer depositing in leather, presented in the previous sections, together with that of other (BA + MMA, BA) polymer-leather composites, are correlated with their liquid water absorptivities in the sections remaining. Imbibition of water by composites of cotton⁴³ and wool^{5,44} showed little difference compared to that by untreated fibers, when the data were corrected to pure substrate. Classical water vapor sorption studies also revealed that while a decrease in adsorption was exerted by polystyrene on wood pulp cellulose,⁴⁵ little effect was found for polyacrylonitrile on cellophane.⁴⁶ However, grafted polystyrene branches on cotton fiber actually increased regains substantially with the extent of grafting.⁴⁷ In contrast, some isotherms of wool composites were shifted vertically below the curves of pure wool,^{44,48} while other composites showed either no effect⁵ or an increase in regain if the branch was water soluble.⁴⁹ Water vapor transmission of acrylate composites of leather showed decreased transmission with polymer content,⁵⁰ probably reflecting tortuosity restrictions or diffusive retardation of water vapor transport. Equilibrium water absorptions³⁴ increased, however, when corrected to neat leather.^{50,51}

Liquid Water Absorption in Controls and Composites

All the results on rate and equilibrium bulk water absorption obtained in this work for both the composites and their respective controls are summarized in Table III. The rate data were selected from the more revealing time increments of plots of typical data shown in Figure 19. Thus, the listed time periods summarize the main features of their rate curves and so enable rough reproductions of curves to be made for each listed experiment, as well as permit a qualitative comparison of the reaction dynamics for all systems studied. The quantities v_f , w_{so} , t_{eq} , and w_{max} are explained as follows.

For the linear relations in Figure 19 (data for controls), the rate of change of the weight fraction of water, w_s , with time is

$$w_s = w_{si} + k \ln t \quad (15)$$

TABLE III
Rates and Equivalent Water Absorptions of Selected Polymer-Leather Composites and their Controls

Experiment No.	Type of system	w_2^a	ν_f^b	Rates of water absorption ^c				Equilibrium absorption ^f		
				w_{s0}^d 5 sec	w_s 10 min	w_s 8 days	t_{eq}^e min	w_{s0}	w_{max}	w_{max}/w_{s0}
Methyl Methacrylate-Leather Composites and their Controls										
1	emulsion	0	0.634	0.520	0.559	0.559	0.08	0.632	0.605	0.958
2 ^g	emulsion	0.182	0.577	0.536	0.570	0.605	0.08	0.575	0.556	0.967
3	emulsion	0	0.629	0.570	0.594	0.626	0.08	0.627	0.626	0.999
4 ^g	emulsion	0.347	0.467	0.300	0.550	0.593	3.2	0.466	0.488	1.05
5	bulk	0	0.619	0.460	0.510	0.563	0.08	0.617	0.563	0.912
6 ^g	bulk	0.188	0.420	0.240	0.440	0.494	3.2	0.418	0.442	1.06
7	bulk	0	0.587	0.463	0.510	0.565	0.08	0.585	0.564	0.965
8	bulk	0.397	0.127	0.175	0.205	0.339	1645	0.127	0.236	1.867
<i>n</i> -(butyl Acrylate-co-Methyl Methacrylate)-Leather Composites and their Controls										
9	emulsion	0	0.645	0.503	0.550	0.611	0.08	0.643	0.611	0.951
10	emulsion	0.189	0.529	0.040	0.550	0.591	5.2	0.527	0.541	1.03
11	emulsion	0	0.644	0.520	0.565	0.625	0.08	0.641	0.625	0.975
12	emulsion	0.304	0.482	0.200	0.525	0.590	5.2	0.480	0.500	1.04
13	bulk	0	0.597	0.565	0.613	0.651	0.08	0.595	0.651	1.10
14	bulk	0.174	0.425	0	0.510	0.570	30.1	0.427	0.522	1.22
15	bulk	0	0.603	0.510	0.550	0.602	0.08	0.601	0.602	1.00
16	bulk	0.310	0.254	0	0.130	0.480	2713	0.253	0.388	1.54
<i>n</i> -Butyl Acrylate-Leather Composites and their Controls										
17	emulsion	0	0.591	0.483	0.530	0.581	0.08	0.589	0.581	0.987
18	emulsion	0.208	0.521	0	0.300	0.527	63.8	0.520	0.469	0.902
19	emulsion	0	0.583	0.460	0.504	0.555	0.08	0.581	0.555	0.955
20	emulsion	0.303	0.480	0	0.440	0.525	30.1	0.478	0.435	0.910
21	bulk	0	0.565	0.490	0.535	0.594	0.08	0.563	0.594	1.06
22	bulk	0.143	0.450	0	0.120	0.433	4472	0.448	0.396	0.884
23	bulk	0	0.565	0.457	0.503	0.558	0.08	0.565	0.567	0.984
24	bulk	0.281	0.283	0	0.095	0.408	4472	0.243	0.284	1.17

^a Weight fraction of polymer in the composite. Controls are $w_2 = 0$.

^b Eq. (20).

^c Based on 100% leather.

^d Intercept of curve-fitted data at 1 sec; approximately the same in 5 sec, which is the end of the initial rapid imbibition period.

^e Time to reach steady-state rate, as in Fig. 19.

^f Composites not corrected to 100% leather.

^g Experiments 8, 6, 12, respectively, of Table I.

where w_{si} is the instantaneous (1 sec) weight fraction of water absorbed. This is taken to be the water imbibed instantaneously into the larger pores and capillaries in the leather matrix [Fig. 7(b)]. Experiments correlating volume expansion with water uptake over very short times (increments of 1 sec) for periods of up to 5100 sec yielded constant apparent densities, averaging 1.091 ± 0.014 g cm⁻³, after 2 sec. Consequently, the fibrous matrix expanded almost as rapidly as water was imbibed, even for times approaching w_{si} . The average value of k in eq. (15) for all of the untreated leather samples (taken from computer curve fitting data) in Table III was 0.00670 ± 0.00092 sec⁻¹ (Fig. 19). By use of this constant, rates of imbibition of condensed water into chrome-tanned crust leather can be predicted from two empirical equations. The first of these is

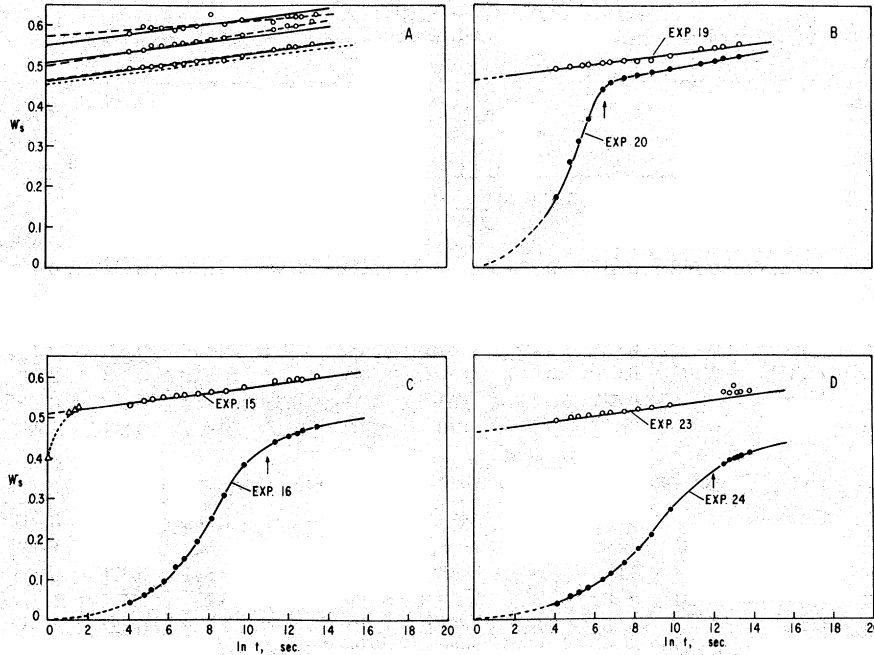


Fig. 19. Rates of water absorption (A) into selected untreated 5-oz chrome-tanned cattlehide panels (controls) and (B)–(D) into various polymer-leather composites and their controls, selected from Table III, respectively. Composite rates drawn based on 100% leather. (—) eq. 16; (---) eq. 17; (---) curve fit.

$$w_s(t) = (w_{sa} - k \ln t') + k \ln t \quad (16)$$

where w_{sa} is the weight fraction of water absorbed by an experimental sample of leather at an arbitrary time, $\ln t'$, up to eight days (30 min used here). The second depends on knowledge of the apparent density, ρ_{ao} , of the starting leather to yield

$$w_s(t) = (w_0 - K\rho_{ao}) + k \ln t \quad (17)$$

where the constants w_0 and K are 0.792 and 0.568, respectively. These constants were obtained by correlating computer-fitted w_{si} values for the control data in Table III with their apparent densities. The solid lines in Figure 19 for the control data were drawn by use of eq. (16); the dotted line is from eq. (17). In general, eq. (16) resulted in far better correlation than that provided by eq. (17), probably because of well-known uncertainty and variation of dry-leather apparent densities.¹

Equations (16) and (17) can be used for evaluating composite data, as well as the untreated leathers just discussed, provided there is little influence of the polymer on the water absorption by the collagen phase. If there is influence, monotonic or sigmoidal curves, such as in Figures 19(B)–19(D), are found. For data correlation with eq. (15) (Table III), all values of w_s for composites were based on pure leather. Because the fraction of water absorbed, f_s , by the fibers of pure leather is given by

$$f_s = [(W_1 + W_s) - W_1]/W_1 = W_s/W_1 \quad (18)$$

where W_s is the weight of water taken up by the sample, f_s/w_1 is the corre-

sponding value for pure leather in the composite. This quantity is related to w_s by

$$f_s/w_1 = w_s/(1 - w_s) \quad (19)$$

Substituting eq. (15) into eq. (19) yields

$$f_s/w_1(t) = w_{si} + k \ln t/[1 - (w_{si} + k \ln t)] \quad (20)$$

From the composite densities¹ $1/V_t$, eq. (1), the volume fraction of free space is

$$v_f = v_{f0}(W_1/\rho_{a0})/[v_{f0}(W_1/\rho_{a0}) + W_2/\rho_p + W_1/\rho_r] \quad (21)$$

Since this is the space involved in matrix expansion that resulted in the constancy of the wet densities just shown, it follows that the limiting water sorption weight fraction $w_{s0} = v_f \rho_w$, where ρ_w is the density of liquid water at ambient temperature. In eq. (15) the maximum weight fraction of water absorbed, w_{smax} , is approached at long times (in this work eight days). Consequently, the ratio (w_{smax}/w_{s0}) relates equilibrium absorptivity to the initial volume fraction of free space for the composites and their controls. Three conditions are pertinent (Table III). When w_{smax}/w_{s0} is unity the expected balance between volume expansion and equilibrium absorptivity is maintained. If $w_{smax}/w_{s0} < 1$ some fiber sites continue to be protected by polymer, even at very long times. In contrast, when $w_{smax}/w_{s0} > 1$, the fiber matrix is exposing new sites or unpredictable new capillary space is opened for water deposition. In this work, f_{smax} for an average of the controls was 1.415 ± 0.152 . This agrees with a value of 1.451 of the previous article¹ for wet volume expansion of composites. This agreement indicated little long-time diminution of water absorption ability of the leather in the cited¹ composite materials.

Table III shows that most of the rate data for composite samples lay close to the rates for their controls. For the emulsion systems, some perturbation occurred at very short times (≤ 10 min) (experiments 4, 12, 18, and 20). The existence of polymer-free layers in these systems probably influenced their rapid adsorption rates. In support of this idea, homogeneous bulk and solution systems all showed short time retardations and some (experiments 6, 8, 16, 22, and 24) continued to show reduced absorption even after eight days (Fig. 19). This seems surprising because the micrographs showed qualitatively similar morphologies for all systems.

Under equilibrium conditions in the emulsion systems, the leather portion eventually absorbed its full complement of water, because w_{smax}/w_{s0} was close to unity in Table III. However, the bulk and solution systems show anomalies. Only one (experiment 22) resulted in a reduced value for the ratio. Many (experiments 8, 14, 16, and 24) showed values considerably greater than unity, even though the corresponding rate data (column 7) indicated less absorption than for the controls. The fault appears to lie in the magnitude of the theoretical value of w_{s0} . The theory¹ was conceived on the assumption that the gross free space in the matrix would be filled rapidly by polymer in the prevailing unhydrated fiber network. However, unless protection is great, both monolayer and capillary water absorption⁵² occur, permitting water entrance into the fine voids⁵³ present in fibrils so as to produce normal leather plumping. Because the micrographs of Figure 18 show that polymer did not penetrate to the vicinity of fibrils in a bulk

system, this expansion will be only marginally restricted and lead to w_{smax}/w_{s0} greater than unity. In the emulsion systems, the form of the pertinent expression¹ has already accounted for this expansion, so that the ratios in Table III are found to be unity.

Data for the absorption (or evaporation) of a drop of water from the grain surfaces of selected polymer-leather composites are shown in Table IV. The results are self-explanatory except that surface rates were much slower for the emulsion systems than for their corresponding totally immersed composites (Table III). This might again be the influence of the layer deposition, although polymer deposited in the grain composite region [Fig. 10(a)] would naturally reduce absorption locally. It is of interest that even strongly hydrophobic *n*-octadecyl acrylate monomer retards absorption, but that at small ω_2 , poly(*n*-octadecyl acrylate) is only slightly effective.

SUMMARY AND CONCLUSIONS

A better understanding was required of the way that polymer deposited into the fibrous leather matrix, especially by polymerization from a preferred emulsion process developed at this center. The extent of hydrophobicity conferred by the deposited polymer is also important in shoe-upper manufacture. Consequently, light microscope and scanning electron micrographs were obtained on selected methyl methacrylate-leather composites, previously prepared and

TABLE IV
Grain Surface-Water Penetration Rates of Selected Composites

Sample No.	Description	w_2	t^a , sec	t/t_0	Penetration
0	control, average	0	4.42 ^b	1	yes
1	MMA, emulsion ^c	0.0807	5	1.1	yes
2	MMA, emulsion ^c	0.2818	92	20.8	yes
3	BA + MMA, emulsion	0.0875	100	22.6	yes
4 ^d	BA + MMA, emulsion	0.3041	3365	761 ^d	no
5	BA, emulsion	0.0918	130	29.4	yes
6	BA, emulsion	0.2900	3840	869 ^d	no
7	MMA, solution	0.0962	45	10.2	yes
8	MMA, solution	0.2917	2640	597	yes
9	BA + MMA, solution	0.1042	1140	258	yes
10	BA + MMA, solution	0.2932	4140	937 ^d	no
11 ^d	BA, solution	0.1431	3600	815 ^d	no
12	BA, solution	0.2928	3870	876 ^d	no
13	POA ^e , solution	0.0307	17.3	3.90	yes
14	POA ^e , solution	0.0645	30.8	7.60	yes
15	POA ^e , solution	0.2081	>3360	760 ^d	no
16	OA ^e , monomer	0.1969	374	85	yes
17	OA ^e , monomer	0.1322	100	23	yes
18	OA ^e , monomer	0.1731	805	182	yes
19	OA ^e , monomer	0.1227	115	26	yes
20	OA ^e , monomer	0.0854	60	14	yes

^a Time necessary for one standard drop of water to disappear from the grain surface.

^b $t_0 = 4.42$ sec.

^c All emulsion composites extracted with methanol.

^d Experiments 12 and 22 of Table III.

^e *n*-Octadecyl acrylate monomer, OA, or polymer, POA.

characterized,¹ and the kinetics of their preparation in emulsion were investigated.² Negative replicas imprinted in the continuous phase of the isolated polymer were also viewed microscopically. The replicas were prepared by preferential removal of the collageneous material with hot 6N hydrochloric acid. Both types of micrographs for the emulsion deposited composites revealed polymer residing in coarse aggregates, preferentially around individual fibers so that bundles were expanded with continued deposition. The replicas supported this morphology quantitatively but also revealed, in scanning electron micrographs at high magnification, some limited envelopment of fibrils. Residues of partially coagulated polymer particles were found when benzene was omitted as a composite solvent. Micrographs of both composites and replicas, prepared by bulk or solution polymerization, revealed more space filling of the initial composite compared to those prepared in emulsion, but no deposition at all near fibrils. Thus, deeper penetration of depositing polymer occurred under hydrating conditions. In general, the theory defining polymer location in part I and modified here to predict replica properties was supported by the physical properties and morphologies actually found for the replicas. However, the mechanism of expansion of fiber bundles, suggested in part II, appears to be in better correspondence with the experiment. Because micrographs of bound and deposited polymer replicas were identical and the number of entangled polymer coil segmental volumes between attachable sites was great, little support of grafting by the micrographs was forthcoming. Equilibrium absorptions of liquid water by composite and controls were identical for emulsion systems although the composite rates were perturbed. In contrast, both rate and equilibrium absorptivities of the bulk and solution composites were retarded by polymer presence.

The authors thank Mrs. Sandra P. Graham for the computer curve fitting and Mr. Franklin P. Rorer and Mrs. Ruth D. Zabarsky for preparation of the SEM prints.

References

1. E. F. Jordan, Jr., B. Artymyshyn, A. L. Everett, M. V. Hannigan, and S. H. Fearheller, *J. Appl. Polym. Sci.* (part I), **25**, 2621 (1980).
2. E. F. Jordan, Jr. and S. H. Fearheller, *J. Appl. Polym. Sci.* (part II), **25**, 2755 (1980).
3. J. C. Arthur, *Adv. Macromol. Chem.*, Vol. 2, W. M. Pasika, Ed., Academic, New York, London, 1970, pp. 1-87.
4. M. S. Bains, *J. Polym. Sci., Part C*, **37**, 125 (1972).
5. K. Arai, *Block and Graft Copolymerization*, R. J. Ceresa, Ed., J. Wiley, New York, 1973, pp. 193-310.
6. P. J. Nayak, *J. Macromol. Sci. Rev. Macromol. Chem.*, **14**, 193 (1976).
7. J. C. Watt, *J. Macromol. Sci. Rev. Macromol. Chem.*, **5**, 175 (1970).
8. K. Panduranga Rao, K. Thomas Joseph, and Y. Nayudamma, *J. Sci. Ind. Res.*, **29**, 559 (1970).
9. K. Panduranga Rao, K. Thomas Joseph, Y. Nayudamma, and M. Santappa, *J. Sci. Ind. Res.*, **33**, 243 (1974).
10. G. M. Brauer and D. J. Termini, *Adv. Chem. Ser.*, **145**, 175 (1975).
11. K. Panduranga Rao, K. Thomas Joseph, and Y. Nayudamma, *J. Polym. Sci., Part A-1*, **9**, 3199 (1971).
12. K. Panduranga Rao, K. Thomas Joseph, and Y. Nayudamma, *J. Appl. Polym. Sci.*, **16**, 975 (1972).
13. A. H. Korn, S. H. Fearheller, and E. M. Filachione, *J. Am. Leather Chem. Assoc.*, **67**, 111 (1972).

14. A. H. Korn, M. M. Taylor, and S. H. Fearheller, *J. Am. Leather Chem. Assoc.*, **68**, 224 (1973).
15. E. H. Harris, M. M. Taylor, and S. H. Fearheller, *J. Am. Leather Chem. Assoc.*, **69**, 182 (1974).
16. M. M. Taylor, E. H. Harris, and S. H. Fearheller, *J. Am. Leather Chem. Assoc.*, **72**, 294 (1977).
17. H. A. Gruber, E. H. Harris, and S. H. Fearheller, *J. Appl. Polymer Sci.*, **21**, 3465 (1977).
18. E. F. Jordan, Jr., B. Artymyshyn, and S. H. Fearheller *J. Appl. Polym. Sci.* (part IV), to appear.
19. R. Y. M. Huang and W. H. Rapson, *J. Polym. Sci., Part C*, **2**, 169 (1963).
20. T. Landells and C. S. Whewells, *J. Soc. Dyers Colour.*, **71**, 171 (1955).
21. T. Valentine, *J. Textile Inst.*, **47**, T 1 (1956).
22. W. R. Goynes and J. A. Harris, *J. Polym. Sci., Part C*, **37**, 277 (1972).
23. M. L. Rollins, A. M. Cannizzaro, F. A. Blouin, and J. C. Arthur, Jr., *J. Appl. Polym. Sci.*, **12**, 71 (1968).
24. W. M. Kaepfner and R. Y-M. Huang, *Text. Res. J.*, **35**, 504 (1965).
25. F. A. Blouin and J. C. Arthur, Jr., *Text. Res. J.*, **33**, 727 (1963).
26. J. C. Arthur, Jr., and F. A. Blouin, *J. Appl. Polym. Sci.*, **8**, 2813 (1964).
27. J. L. Williams, V. S. Stannett, L. G. Roldan, S. B. Sello, and C. V. Stevens, *Int. J. Appl. Radiat. Isot.*, **26**, 169 (1975).
28. F. A. Blouin, N. J. Morris, J. C. Arthur, Jr., *Text. Res. J.*, **36**, 309 (1966).
29. R. J. Demint, J. C. Arthur, Jr., A. R. Markezich, and W. F. McSherry, *Text. Res. J.*, **32**, 918 (1962).
30. M. Lipson and J. B. Speakman, *J. Soc. Dyers Colour.*, **65**, 390 (1949).
31. M. W. Andrews, R. L. D'Arcey, and J. C. Watt, *J. Polym. Sci., Polym. Lett. Ed.*, **3**, 441 (1965).
32. J. A. Swift, *Chemistry of Natural Protein Fibers*, A. S. Asquith, Ed., Plenum, New York, 1977, pp. 81-146.
33. J. V. Yannas, *J. Macromol. Sci. Rev. Macromol. Chem.*, **7**, 49 (1972).
34. ASTM Standard D530-60T, 1960.
35. T. A. Welo, H. M. Ziifle, and A. W. McDonald, *Text. Res. J.*, **22**, 261 (1952).
36. A. H. Nisson and G. K. Hunger, *Encyclopedia of Polymer Science and Technology*, Vol. 3, H. F. Mark, N. G. Gaylord, and N. Bikales, Eds., Interscience, New York, 1966, pp. 131-226.
37. A. J. Hodge in *Treatise on Collagen*, G. N. Ramachandran, Ed., Academic, New York, 1967, pp. 185-205.
38. E. W. Duck, *Encyclopedia of Polymer Science and Technology*, Vol. 5, H. F. Mark, N. G. Gaylord, and N. Bikales, Eds., Interscience, New York, 1966, pp. 801-859.
39. H. A. J. Battaerd and G. W. Tregear, *Graft Copolymers*, Interscience, New York, 1967, pp. 18, 19.
40. R. W. Lenz, *Organic Chemistry of Synthetic High Polymers*, Interscience, New York, 1967, pp. 711-713.
41. (a) R. M. Fitch and C. S. Tsai, in *Polymer Colloids*, R. M. Fitch, Ed., Plenum, New York, 1971, pp. 73-102; (b) pp. 103-116.
42. C. P. Roe, *Ind. Eng. Chem.*, **60**(9), 20 (1968).
43. C. Hamalainen, H. H. St. Mard, and A. S. Cooper, Jr., *Am. Dyest. Rep.*, **57**, 219 (1968).
44. J. T. Williams, V. Stannett, and A. A. Armstrong, *J. Appl. Polym. Sci.*, **10**, 1229 (1966).
45. P. F. LePoutre, H. B. Hopfenburg, and V. Stannett, *J. Polym. Sci., Part C*, **37**, 309 (1972).
46. N. Geacintov, V. Stannett, and E. W. Abrahamson, *Macromol. Chemie*, **36**, 52 (1959).
47. R. E. Kesting and V. Stannett, *Macromol. Chem.*, **65**, 248 (1963).
48. D. S. Varma and K. R. Sarkar, *Angewandte Macromol. Chem.*, **37**, 177 (1974).
49. J. D. Leeder and A. J. Pratt, *J. Appl. Polym. Sci.*, **11**, 1649 (1967).
50. K. Panduranga Rao, D-H. Karnot, K. Thomas Joseph, M. Santappa, and Y. Nayudamma, *Leather Sci.*, **21**, 2 (1974).
51. K. Panduranga Rao, K. Thomas Joseph, and Y. Nayudamma, *Leather Sci.*, **19**, 27 (1972).
52. J. R. Kanagy, *J. Am. Leather Chem. Assoc.*, **42**, 98 (1947).
53. R. Sanjeevi, N. Ramanathan, and B. Viswanathan, *J. Colloid Interface Sci.*, **57**, 207 (1976).

Received March 26, 1980

Accepted April 16, 1980